Journal of Quantitative Spectroscopy & Radiative Transfer 140 (2014) 58–66

Contents lists available at ScienceDirect

Journal of Quantitative Spectroscopy & Radiative Transfer

journal homepage: www.elsevier.com/locate/jqsrt

Line-shape models testing on six acetylene transitions in the $\nu_1+\nu_3$ band broadened by N_2

Robab Hashemi, Hoimonti Rozario, Chad Povey, Adriana Predoi-Cross *

Alberta Terrestrial Imaging Centre, Department of Physics and Astronomy, University of Lethbridge, 4401 University Drive, Lethbridge, AB, Canada T1K 3M4

ARTICLE INFO

Article history:
Received 7 October 2013
Received in revised form
10 February 2014
Accepted 11 February 2014
Available online 18 February 2014

Keywords:
Spectral line-shapes
Dicke narrowing
Speed dependent effects
Collisional broadening

ABSTRACT

We present a line-shape study of six absorption lines P(21), P(16), P(19), R(16), R(19) and R(21) in the $\nu_1+\nu_3$ band of the acetylene perturbed by nitrogen. The spectra were recorded using a 3-channel diode laser spectrometer. For each transition studied, the N_2-broadening, N_2-narrowing, N_2-pressure induced line shift and N_2-line mixing coefficients were retrieved using several line-shape models. Moreover, we compare the N_2-narrowing parameter to the dynamical friction parameter. The spectra were recorded over a pressure range from 5 to 250 Torr, and were analyzed using the Voigt, Rautian, Correlated Rautian, Galatry, Rautian–Galatry, Speed Dependent Voigt, Speed Dependent Rautian and Correlated Speed Dependent Rautian line-shape models. Furthermore, we have studied the influence of the type of interaction potential in our analysis for line-shape models that take into account speed dependent effects.

1. Introduction

Acetylene was discovered in 1860 and was labeled the "new carburet of hydrogen". Years later it was renamed as "acetylene". Acetylene is a light, simple, linear molecule that has sparked the interest of experimentalists and theoreticians alike. This molecule is present in the atmospheres of many gas giants. It is also present as a trace constituent in stellar atmospheres and in the interstellar medium. Its discovery in planetary atmospheres offers clues to the evolution of those planets. For example, its discovery on Saturn's moon Enceladus suggested catalytic reactions were possible, making it a candidate for prebiotic chemistry [1]. Atmospheric spectra recorded by the Atmospheric Chemistry Experiment (ACE) mission [2] proved that acetylene can be found in trace amounts in the Earth's atmosphere where it plays both the role of the reactant and product for chemical reactions.

The interpretation of planetary atmospheric spectra obtained from aircraft, telescope and spacecraft based spectroscopic remote sensing instruments relies on the availability of accurate line parameters for all atmospheric constituents [3]. In the case of acetylene, of particular importance are accurate line parameters and their temperature dependences needed to assess the suitability of different line-shape models to reproduce the experimental line profiles [4–11].

The line positions for transitions in the $\nu_1+\nu_3$ band are often used as a frequency standard by the telecom industry [12]. The line parameters relevant to spectroscopic studies of Earth and Planetary atmospheres are stored in the HITRAN12 [13] and GEISA [14,15] databases. The pressure broadening of acetylene in the $\nu_1+\nu_3$ band located in the 1550 nm region was first studied in 1960 [16]. Varanasi and Bangaru [17] focused on measuring self- and H_2-broadened line parameters of acetylene. Pine [18] has used a difference frequency laser system to

* Corresponding author. Tel.: +1 403 329 2697; fax: +1 403 329 2057.
E-mail address: Adriana.predoicross@uleth.ca (A. Predoi-Cross).

http://dx.doi.org/10.1016/j.jqsrt.2014.02.013
0022-4073

measure the self-, N_2- and Ar- broadening coefficients for acetylene transitions in the $\nu_1+\nu_5$ band using a Rautian Profile (RP) or hard collision [19] model.

Biswas et al. [20] used the Voigt profile (VP) [21] to measure the self- and N_2-broadening for acetylene transitions in the $\nu_1+3\nu_3$ band using spectra recorded with a diode laser spectrometer working nearby 782 cm^{-1}. Diode laser spectroscopy was also employed by Yelleswarapu and Sharma [22] in their study of self-broadening and pressure induced self-shifts for transitions in the $\nu_1+3\nu_3$ band using the Voigt profile.

Povey et al. [23,24] have measured 20 lines in the $\nu_1+\nu_2+\nu_4+\nu_5$ band of acetylene and examined the effects due to temperature and pressure changes. A selection of six pressures has been chosen and for each pressure seven temperatures were used ranging from 213 K to 350 K using VP [21] and Speed Dependent Voigt profile (SDV) [25]. Moreover, the authors have obtained N_2- and self-broadened for six transitions of acetylene in the $\nu_1+\nu_3$ and over a range of temperatures recorded by 3-channel diode laser spectrometer. They have examined the spectra using RP [19].

N_2-broadened line widths and pressure induced line shifts have been measured by Rozario et al. [26] for transitions in the $\nu_1+\nu_3$ band over the 213–333 K temperature range. The VP and RP were used to retrieve line parameters.

Twenty acetylene transitions belonging to the $\nu_1+3\nu_3$ band have been studied in detail by Valipour and Zimmerman [27] for mixtures of acetylene and different broadeners: N_2, O_2, air, He, Ne, Ar, Kr, Xe using the Galatry Profile (GP) or soft collision model [28] and RP. A study of the $\nu_4+2\nu_5$ band located in the 5 μm range was performed by Jacquemart et al. [29] using the RP profile. More recently, ten self-broadened P-branch transitions in the $\nu_1+\nu_3$ band of acetylene have been studied by Li et al. [30] using diode laser spectroscopy and fitting with VP and RP.

Fissiaux et al. [31] have measured the N_2-broadening coefficients at room temperature for twelve transitions of C_2H_2 in the $\nu_4+\nu_5$ band. The collisional widths have been individually retrieved using the VP, RP, GP and Speed Dependent Rautian (SDR) [32] line-shape models.

Devi et al. [33] and Podolske et al. [34] have measured the N_2-broadening coefficients of C_2H_2 in the $\nu_1+3\nu_3$ band using diode-laser spectroscopy and VP fits. Lambot et al. [35] studied transitions in the ν_5 band using spectra recorded with a diode-laser spectrometer and spectral fits using RP.

Diode laser spectroscopy was used by Dhyne et al. [36] to measure the N_2-broadening and N_2-shift coefficients for nine transitions R(5), R(11), P(8), P(10), P(12), P(14), P(16), P(21) and P(23) in the $\nu_{4+}\nu_5$ band of C_2H_2 recorded over a 173.2 to 298.2 K temperature range. The broadening coefficients were obtained from fits with the VP, RP and GP.

In this work, we have measured N_2-broadening coefficients of C_2H_2 at room temperature for six transitions in the R and P-branch of the $\nu_{1+}\nu_3$ band using our 3-channel diode-laser spectrometer. We have recorded spectra at pressures between 5 and 250 Torr for each line of interest. The spectra recorded below 40 Torr as intermediate pressure range have been analyzed using the VP, RP, GP, Rautian–Galatry Profile (RGP) [37] and Correlated Rautian (CR) profiles. For the entire pressure range, we have tested the applicability of the SDV, SDR and CSDR [38] line-shape models. Except for VP, Dicke narrowing [39] effect has been considered in all mentioned line-shape models. The experimental results for the narrowing parameters have been compared with calculated values based on the theory of diffusion.

For each line the spectra recorded over the entire pressure range were analyzed using the SDV, SDR and CSDR line-shapes and an asymmetric line mixing component. Overall, we have investigated a wide range of line-shape models to test how closely they can reproduce the observational spectra in different pressure ranges. We have also taken into account the effect of the interaction potential to the form of inverse power on the spectral line-shape profiles to see if different values of the potential power will alter the retrieved line parameters.

2. Experimental details

A 3-channel tunable diode laser spectrometer described in detail in an earlier publication from our group [23] was used to record all spectra needed for the present study. A brief discussion of the main features of the experimental setup follows. The first channel of the diode laser spectrometer contains a single pass, temperature and pressure controlled cell of 1.54 m optical path, filled with the sample gas mixture. The second channel contains a room temperature reference cell of 1.5 m optical path, filled with pure gas and used to record reference spectra. The third channel records the signal from the laser system, i.e. the background signal. The optical signals were detected using 3 InGas detectors and preamplifiers. A LabView based data acquisition system allowed us to record spectra in the 1500 to 1570 nm range with a signal to noise ratio more than 2000:1. A combination of a Fabry Perot cavity and a WA-1500 EFXO wavemeter were used to measure the wavelength accurately.

The gas temperature was measured at different depths inside the cell mounted on channel 1, using five platinum resistor thermometers mounted on rods of different lengths, and a Lakeshore temperature sensor monitor. The temperature stability along the cell was within 0.3 K [23]. The mixture of acetylene and N_2 was supplied by Praxair with a quoted concentration of 9.94%. The gas pressures for the cell on channel 1 were measured using two MKS Baratron pressure gauges with full scale readings and a MKS signal conditioner model 670. Recording from 5 to 40 Torr have been carried out using the 0–100 Torr pressure gauge. The pressures in the 100 to 250 Torr range were measured using the 0–1000 Torr pressure gauge. The line positions of the transitions are calibrated using data available in the HITRAN12 database [13].

The spectral lines were modeled and analyzed using a multi-spectrum fit software [40] that takes into account the instrumental line-shape of our laser spectrometer [23]. In this study, we have recorded room temperature spectra at eleven different pressures between 5 and 250 Torr for the P(21), P(19), P(16), R(16), R(19) and R(21) transitions in the $\nu_1+\nu_3$ band of acetylene. The experimental conditions for all spectra used in this study are available in Table 1.

Table 1
Experimental conditions for the spectra used in this study (concentrations of saturated lines are not presented).

Total gas pressure (Torr)	Concentration percentage					
	P21	P19	P16	R16	R19	R21
5	9.332	9.346	9.406	9.656	9.186	9.487
5	9.399	9.472	9.477	9.552	9.254	9.390
5	9.395	9.369	9.456	9.534	9.217	9.421
5	9.468	9.430	9.452	9.534	9.271	9.376
10	9.274	9.186	9.416	9.950	9.285	9.472
10	9.311	9.135	9.379	9.569	9.295	9.347
10	9.284	9.187	9.477	9.557	9.281	9.378
10	9.295	9.127	9.376	9.482	–	9.466
20	9.313	9.294	9.262	9.427	9.076	9.227
20	9.223	9.317	9.408	9.314	9.153	9.178
20	9.253	9.207	9.284	9.407	9.076	9.119
20	–	9.291	–	9.415	8.999	9.289
30	9.272	9.450	9.478	9.370	9.091	8.927
30	9.413	9.239	9.382	9.317	8.929	9.055
30	9.432	9.405	9.308	9.269	9.008	9.147
30	9.463	9.296	9.288	9.277	8.979	–
40	9.412	9.617	9.469	9.256	8.775	9.011
40	9.568	9.618	9.639	9.138	8.775	8.947
40	9.440	9.678	9.564	9.142	8.775	8.767
40	9.513	9.716	9.372	9.595	–	8.990
100	–	–	–	9.552	–	9.210
100	–	–	–	9.655	–	9.160
200	–	–	–	9.552	9.216	8.930
200	–	–	–	9.533	9.271	7.949
200	–	–	–	8.770	7.883	8.854
200	–	–	–	8.847	8.069	8.690
225	–	–	9.590	8.451	8.590	8.436
225	–	–	–	8.675	8.176	8.548
225	–	–	–	8.633	8.265	8.398
225	–	–	–	8.653	8.364	8.863
250	–	–	–	8.500	7.768	9.047
250	–	–	–	9.210	7.840	9.942
250	8.976	–	–	8.715	8.008	9.924
250	8.976	–	9.930	9.798	8.177	9.914

3. Spectroscopic analysis

3.1. Line profiles

To achieve an accurate modeling of the recorded absorption line-shapes, we must consider different physical effects including the pressure broadening, line narrowing, shifting, effects of molecular speed dependence, and line mixing effects. Therefore, choosing the appropriate line-shape function plays an important role in the interpretation of observed spectra for different molecular species and in the retrieval of line-shape parameters for different applications. Most often, for remote sensing applications the Voigt profile is used. VP is a fast and common way to analyze remote sensing spectra. However, it is not reliable enough for reproducing the observed spectra recorded with a very high signal to noise ratio.

The experimental absorbance $\alpha(\tilde{\nu})$ can be obtained using the Beer–Lambert's law as

$$\frac{I_t(\tilde{\nu})}{I_0(\tilde{\nu})} = \exp[-\alpha(\tilde{\nu})], \tag{1}$$

where $I_t(\tilde{\nu})$ and $I_0(\tilde{\nu})$ are the transmitted intensities through the sample gas cell under vacuum at wavenumber $\tilde{\nu}$ (cm^{-1}). By fitting a theoretical line-shape to the measured absorbance, the line parameters can be retrieved. First, the VP can be defined by

$$\alpha_v(A,x,y) = A\frac{y}{\pi}\int_{-\infty}^{+\infty}\frac{\exp(-t^2)}{y^2+(x-t)^2}dt = A\mathrm{Re}[W(x,y)], \tag{2}$$

The $W(x,y)$ function and parameters x, y and A are defined by below equations

$$W(x,y) = \frac{i}{\pi}\int_{-\infty}^{+\infty}\frac{\exp(-t^2)}{x+iy-t}dt, \tag{3}$$

$$A = \frac{S\sqrt{\ln 2}}{\gamma_D\sqrt{\pi}},\ y = \sqrt{\ln 2}\frac{\gamma_C}{\gamma_D},\ x = \sqrt{\ln 2}\frac{\tilde{\nu}-\tilde{\nu}_0}{\gamma_D} \tag{4}$$

here S is the line intensity, $\tilde{\nu}_0$ (in cm^{-1}) is the line center wavenumber, γ_C is the collisional half-width of C_2H_2 diluted in N_2, and γ_D is the theoretical Doppler half-width given by

$$\gamma_D = 3.581\times10^{-7}\tilde{\nu}_0\sqrt{\frac{T}{M}}, \tag{5}$$

where T is the temperature in Kelvin and M is the molecular mass in atomic mass unit. The Doppler half-width was found to be 0.0796 $\mathrm{cm}^{-1}$for the R(16) transition at room temperature.

We used the RP and GP providing one more parameter β_C (in cm^{-1}) to introduce the collisional narrowing due to the molecular confinement. The hard collision model of RP can be written as

$$\alpha_R(x,y,z) = A\mathrm{Re}\left[\frac{W(x,y+z)}{1-\sqrt{\pi}zW(x,y+z)}\right], \tag{6}$$

In the Eq. (6) the parameters A, x and y are the same as defined by Eq. (4). The parameter z is given by

$$z = \sqrt{\ln 2}\frac{\beta_C}{\gamma_D}. \tag{7}$$

The GP can be defined by Eq. (8) with the same definition of the parameters as for the RP model.

$$\alpha_G(x,y,z) = \frac{A}{\sqrt{\pi}}\mathrm{Re}\left[\int_{-\infty}^{+\infty}\exp\left(-ixt-yt-\frac{zt-1+e^{-zt}}{2z^2}\right)dt\right], \tag{8}$$

The measured collisional narrowing coefficient (β_C) has been also compared to the dynamical friction parameter β_{diff} (in $\mathrm{cm}^{-1}\,\mathrm{atm}^{-1}$) of the Brownian motion, expressed as [41]

$$\beta_{\mathrm{diff}} = \frac{k_BT}{2\pi cMD}, \tag{9}$$

where, k_B is the Boltzmann constant, T (in K) is the temperature, c (in m/s) is the light velocity, M is the molecular mass in atomic mass unit and D (in $\mathrm{cm}^{-2}\,\mathrm{s}^{-1}$) is the optical diffusion coefficient for the C_2H_2–N_2 system.

The dependence of collisional broadening on the different absorber speeds was accounted for the first time by Berman [42] and later by Ward et al. [25] and Pickett [43]. These authors introduced the SDV line-shape model which describes the dependence of relaxation parameter, Γ, on the absorber speed, v_a.

The semi-empirical quadratic form of Rohart et al. [44,45] for $\Gamma(v_a)$, is often used and leads to an analytical

correlation function:

$$\Gamma(v_a)=\Gamma_0+\Gamma_2\left[\left(\frac{v_a}{v_{a0}}\right)^2-\frac{3}{2}\right] \tag{10}$$

$$\Phi_{SDV}(t)=\frac{\exp[-iw_0t-(\Gamma_0-3\Gamma_2/2)t]}{(1+\Gamma_2t)^{3/2}}\exp\left[-\frac{(kv_{a0}t)^2}{4(1+\Gamma_2t)}\right] \tag{11}$$

In these equations, the phenomenological parameter $\Gamma_0=\langle\Gamma(v_a)\rangle$ is the mean relaxation parameter over absorber molecular speeds v_a, Γ_2 is a parameter describing the speed dependence of the relaxation parameter $\Gamma(v_a)$, and v_{a0} is the most probable speed of the absorbing molecule. Both Γ_0 and Γ_2 are expected to have a linear dependence with pressure. The retrieved broadening coefficients $\gamma=\Gamma_0/p$ are independent of pressure.

In testing the speed dependent effects, we used the SDR profile which has been developed by Lance et al. [32]. In addition, we have considered a fully correlated model to fit our measurements of N_2-broadened C_2H_2. Joubert et al. [46] have studied the RP model in the case of strong collisions, where the line-shape parameters are independent of speed. In testing these profiles, we have fixed the narrowing parameter and taken into account the line-mixing effects that are important in the high pressure regime.

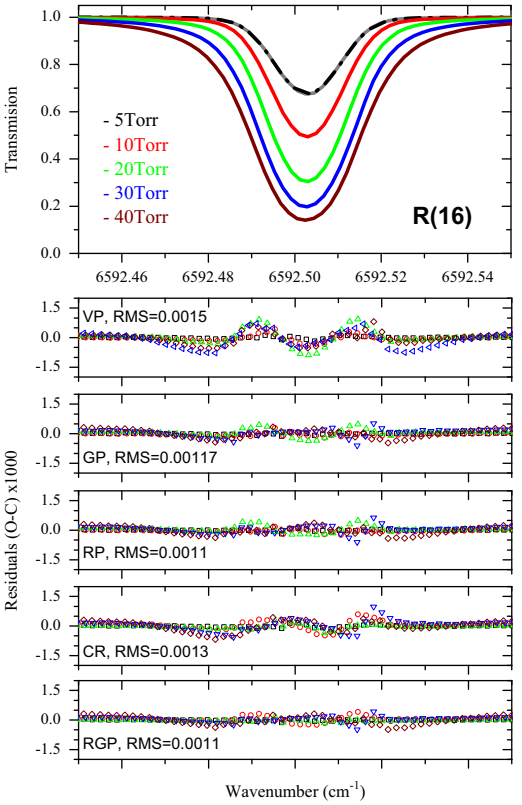

Fig. 1. The transmission spectrum of the R(16) line of C_2H_2–N_2 at pressures 5–40 Torr and 296 K. Residuals (O−C) under these conditions resulting from least squares multi-spectrum fittings of experimental data to the VP, RP, GP, RGP and CR line-shape models (Bottom panels).

Using a multi-fit program that has all these theoretical models implemented, we can fit simultaneously spectra recorded for each line of interest at different pressures and

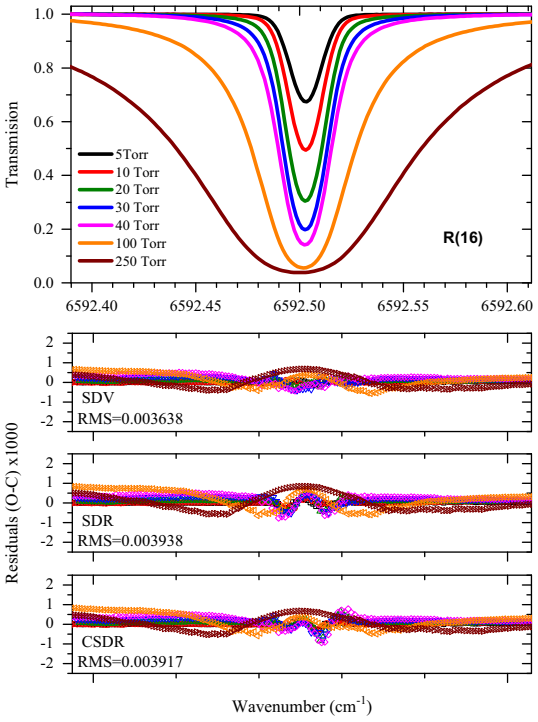

Fig. 2. The transmission spectrum of the R(16) line of C_2H_2–N_2 at entire pressure range (5–250 Torr) and 296 K. Residuals (O−C) have fitted using SDV, SDR and CSDR line-shape models.

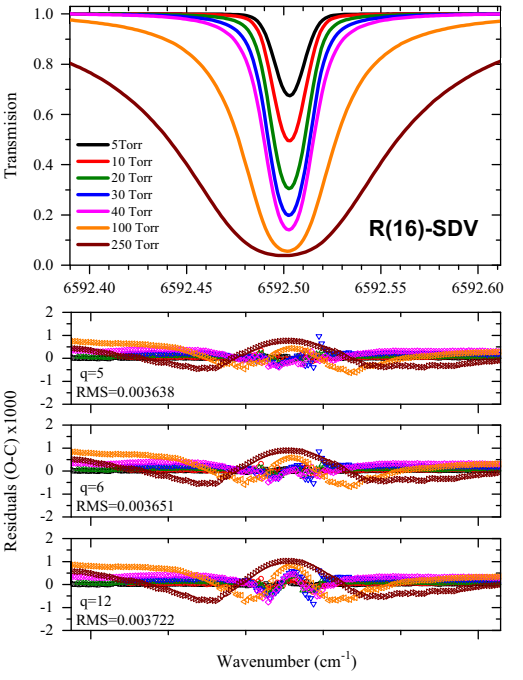

Fig. 3. The measured profile for the R(16) line of C_2H_2 perturbed by N_2 fitted with SDV model with three values for potential power ($q=5$, $q=6$ and 12) at pressure 5–250 Torr.

at the same temperature to retrieve the line-shape parameters. The mixture of C_2H_2–N_2 used was supplied with a quoted concentration of 9.94%. To have more accurate values of the gas concentration for each spectrum we have fitted the spectral profiles using the line parameters from the HITRAN12 database [13], first and the Voigt profile. Furthermore we have used the retrieved values for concentration in our fits using different line-shape models.

Fig. 1 shows the spectra of the R(16) line of the $\nu_1+\nu_3$ band measured at 296 K. The lower panels show the residuals (Observation − Calculation) × 1000 plotted for several line profiles fitted to the data. Each of the lower panels is plotted with the same vertical scale to make it easier to compare them. Fitting with the VP we get a "*w*"-shaped residual indicating that we are in the Dicke narrowing regime. Fitting the data using the RP and GP, we get an improved result because the Dicke narrowing is taken into account in the formulation of the GP, RP, CR and RGP. Both the RP and GP models lead to very similar residuals as shown for example by the RMS value of the fits. We used the RGP to fit our profiles because for our system the molecular masses for the absorber and perturber involved in either "soft" or "hard" collisions are nearly identical (the mass ratio of C_2H_2/N_2 is equal to 0.93). The residuals obtained for RGP show an improved result as compared with those retrieved using each of the RP, GP and CR. However, we can still observe a small asymmetric structure near the line center. The GP, RP, CR and RGP are all symmetric profiles and cannot reproduce the small asymmetric feature observed for spectra recorded in the 5–40 Torr range. We interpret this small asymmetry in the fit residuals as being evidence of speed dependence effects in our spectra. Based on our fit residuals, we note that the CR model does not offer better results than the RP model.

Fig. 2 presents the results of fitting our spectral profiles recorded at different pressures to the SDV, SDR and CSDR profiles. In the implementation of the SDV profile, the broadening and shift are assumed to depend on collisional speed, and on the inverse power law expression for the inter-molecular potential energy surface. As it is clear from the fit residuals, the CSDR model reproduces the experimental spectra better than the SDR model because it takes into account the collisions between speed dependence and velocity changes. However, based on what Ngo et al. [47]

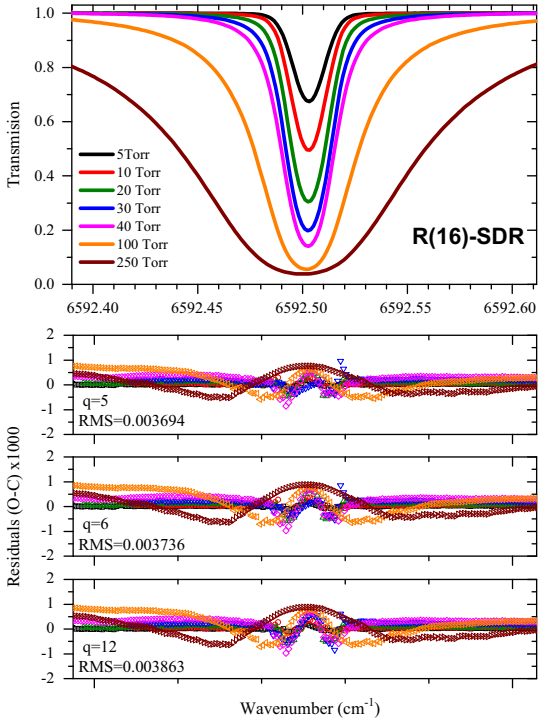

Fig. 4. The measured profile for the R(16) line of C_2H_2 perturbed by N_2 fitted with SDR model with three values for potential power ($q=5$, $q=6$ and 12) at pressure 5–250 Torr.

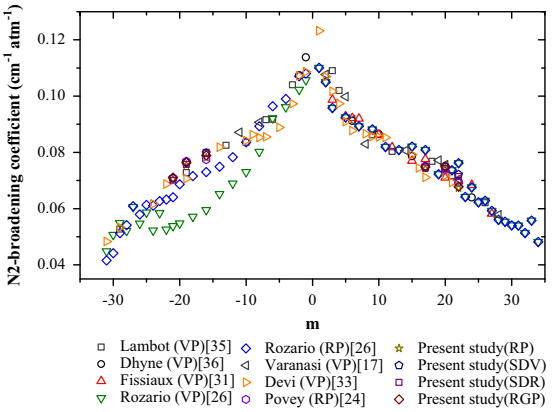

Fig. 5. The retrieved broadening parameter in cm^{-1} atm^{-1} for the six lines of C_2H_2 perturbed by N_2 and their comparison with some published results.

Table 2
N_2-broadening coefficients $\gamma^0_{N_2}$ (cm^{-1} atm^{-1}) at 296 K. Results are derived from the RP, GP, RGP, CR, SDV, SDR, CSDR and VP line-shapes (error values quoted in parentheses correspond to one standard deviation).

Broadening (cm^{-1} atm^{-1})	P(21)	P(19)	P(16)	R(16)	R(19)	R(21)
RP	0.0704(2)	0.0755(4)	0.0781(1)	0.0742(2)	0.0744(2)	0.0673(2)
GR	0.0707(2)	0.0764(3)	0.0793(1)	0.0754(2)	0.0751(2)	0.0690(2)
RGP	0.0710(2)	0.0764(3)	0.0789(1)	0.0748(2)	0.0749(2)	0.0678(2)
CR	0.0705(2)	–	0.0782(2)	0.0747(2)	0.0744(2)	0.0693(1)
SDV	0.0709(4)	0.0765(3)	0.0798(3)	0.0748(4)	0.0750(2)	0.0721(5)
SDR	0.0701(4)	0.0757(3)	0.0795(2)	0.0744(5)	0.0742(2)	0.0714(5)
CSDR	0.0702(4)	0.0756(3)	0.0795(2)	0.0748(4)	0.0738(2)	0.0715(5)
VP	0.0694(4)	0.0768(4)	0.0783(3)	0.0751(5)	0.0754(2)	0.0724(4)

obtained, the partially correlated models reproduce the spectra better than the fully correlated models.

Among all line-shape models considered in our study, it seems that the SDV profile is able to reproduce the observed data at all the tested pressures in this experiment. The RGP reproduces the spectra over a limited pressure range, while the SDV profile, which can be considered as the simplest line-shape that shows speed dependent effects (for example, SDR and CSDR) can reproduce the experimental line profiles with good accuracy.

3.2. Influence of molecular interaction potential shape on line-shapes

Berman [42] and Pickett [43] have shown that the collisional broadening has an inverse power law dependence on the relative speed of the active molecule and the perturber's speed:

$$\gamma(\nu) = a\nu^{P} \tag{17}$$

where the power exponent P is $P=(q-3)/(q-1)$. Here q is the exponent used in the expansion of the isotropic part of the absorber–perturber interaction potential. The simplified isotropic inverse power law interaction potential can be written as [43]

$$V_{\mathrm{iso}}(r) \cong r^{-q} \tag{18}$$

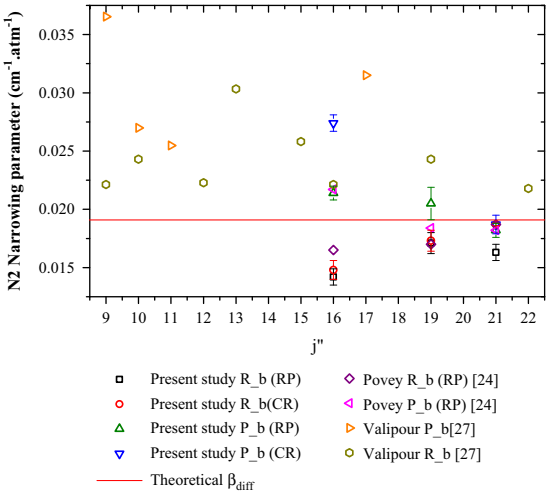

Fig. 6. The retrieved narrowing parameter in $cm^{-1}\,atm^{-1}$ for the six lines of C_2H_2 perturbed by N_2 and their comparison with some published results for RP and CR profiles. The calculated theoretical value of $\beta_{diff}=0.0191\ cm^{-1}\,atm^{-1}$. P_b shows P branch and R_b shows R branch.

where r is the intermolecular distance and the exponent value is adjustable. We have considered the SDV, SDR and CSDR profiles with three different fixed values for the term q in our software. Our software was not capable of fitting for the q parameter. We performed our spectral fits using three values for q, namely 5, 6 and 12. Within experimental errors, the observed profiles were symmetrical. We fixed the narrowing parameters to the values obtained from the analysis of intermediate pressure spectra.

For example, in Figs. 3 and 4 we presented the fit residuals obtained for R(16), which is a well isolated line, using the SDV and SDR profiles. To show the influence of the different values of q on the fitted residuals we plotted them over a range of pressures from 5 to 250 Torr. The fit residuals are minimized for a value of q equal to 5.

From the line-shape parameters and residuals that we obtained, it is clear that the presence of speed dependent collisional broadening leads to the enhancement of the potential type influence on the line-shape and that this influence increases with the increase of the mass ratio [48].

When we fit with SDV, SDR and CSDR models, the $q=5$ gives a slightly smaller residual because the mass ratio for the absorber and perturber is close to one and this value of mass ratio has less influence on potential type. Therefore, the residuals spread closely around the zero level. As a measure of the goodness of each multi-spectrum fit, we have considered the Root Mean Square (RMS) values.

3.3. Retrieved line parameters

Using the initial values taken from [23,24,26] for line parameters, multi-spectrum fits were performed on the set of spectra recorded for different pressures and the same temperature. The software uses non-linear least square fitting to optimize the line parameters by minimizing the residuals between the measured and modeled spectra. Table 2 contains our results for the line broadening coefficients and their errors obtained using different line-shape models.

We combined all the broadening values in one table to be able to compare parameters retrieved with the selected line-shape models in lower pressure regime with line parameters retrieved over the entire pressure range, i.e. using the SDV profile. We also plotted the broadening parameters as a function of m, and compared them with the results of previous studies. As can be seen in Fig. 5, the broadening coefficients decrease with increasing values of $|m|$, as expected. Based on our results we can say that the models that include the speed dependent effects give

Table 3
N_2-narrowing coefficients $\beta^0_{N_2}$ ($cm^{-1}\,atm^{-1}$) at 296 K (results are derived from the RP, GP, RGP and CR line-shapes).

Narrowing ($cm^{-1}\,atm^{-1}$)	P(21)	P(19)	P(16)	R(16)	R(19)	R(21)
RP	0.0182(6)	0.0205(14)	0.0214(6)	0.0142(7)	0.0171(9)	0.0163(7)
GP	0.0236(8)	0.0253(16)	0.0294(7)	0.0246(10)	0.0209(11)	0.0222(9)
RGP	0.0226(7)	0.0284(16)	0.0216(6)	0.0181(9)	0.0199(10)	0.0200(9)
CR	0.0187(8)		0.0274(7)	0.0148(8)	0.0173(9)	0.0187(0)

similar values for broadening parameters, with discrepancies in the 0.5–1% range. However, comparing to the results retrieved at lower pressures with models like the RP model, their difference is around 7%. Normally, for heavier perturbers we expect the retrieved broadening parameters obtained using the VP to be smaller than those obtained using the SDV. Here, because the mass of absorber is comparable with mass of perturber, there is no considerable difference in broadening parameters obtained with the two models.

The results for the retrieved narrowing coefficients are listed in Table 3. The results show that the spectra recorded at pressures below 40 Torr are best modeled by the RGP and the obtained values for narrowing using this model are more or less in between of narrowing parameters obtained using the RP or GP and retrieved values for RP and GP are different. Also, we have compared the calculated the mass diffusion coefficient to the retrieved friction coefficient at 296 K.

The mass diffusion coefficient for a gas mixture can be obtained using the below equation [41,49]

$$D_{12} = \frac{\varepsilon_D k_B{}^{3/2}}{\sqrt{\pi} p \sigma_{12}^2 \Omega_{12}^{(1,1)}(T_{12})} \sqrt{T^3 \frac{(M_1+M_2)}{2M_1M_2}} \tag{19}$$

where M_1 and M_2 are the molecular weights of C_2H_2 and N_2, respectively; T is the temperature in Kelvin; p is the pressure in atmospheres; $\varepsilon_D=3/8$ as shown in T_{12} is a reduced temperature equal to k_BT/ε_{12}; ε_{12} is the depth of the isotropic potential; and is the finite distance at which the intermolecular isotropic potential is zero. From the ab initio PES values of Ref [50], we have $\varepsilon_{12}=88.8\ cm^{-1}$ and $\sigma_{12}=4.015$ Å. In Eq. 19, $\Omega_{12}^{(1,1)}$ is a dimensionless reduced collision integral as a function of the reduced temperature. We obtained D_{12} to be $0.255\ cm^{-2}\ s^{-1}$. We plotted these results in Fig. 6 together with theoretical value of β_{diff} and compared them with obtained results by Povey et al. [24] for R branch transitions and Valipour et al. [27] results for P and R branch. This graph shows that the obtained narrowing parameters are lower than β_{diff} value.

The results for the pressure induced shift coefficients are given in Table 4. For all tested models we obtained negative line shift coefficients. The absolute values of the coefficients increase with increasing values of J as it is shown in Fig. 7. These results are in good agreement with published results by Rozario et al. [26] and little higher than what Valipour et al. [27] obtained.

In this study we also accounted for the line mixing effects observable at higher pressures and the results are presented in Table 5. Line mixing has a dominating effect

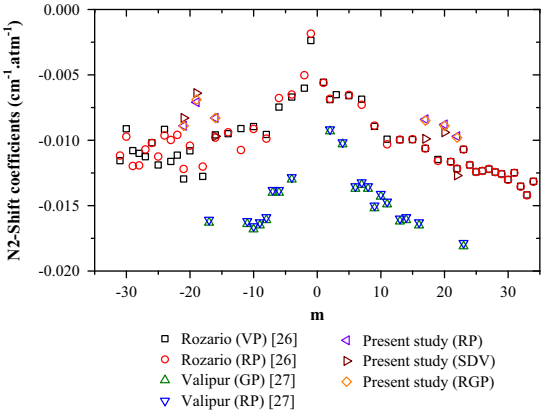

Fig. 7. The retrieved shift parameter in $cm^{-1}\ atm^{-1}$ for the six lines of C_2H_2 perturbed by N_2 and their comparison with some published results.

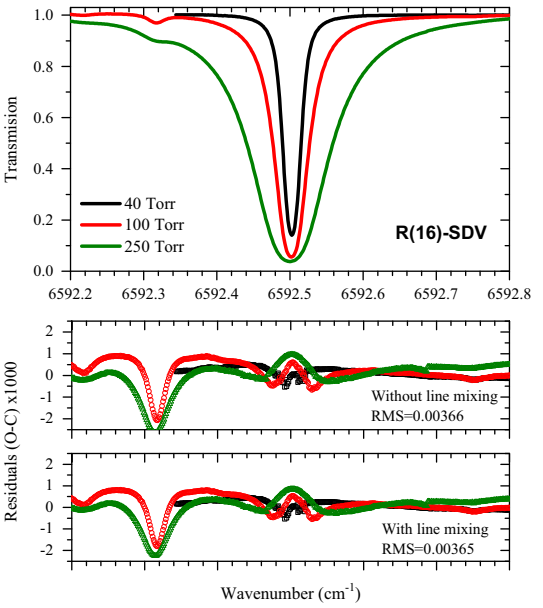

Fig. 8. The line mixing effect for the R(16) line of C_2H_2 perturbed by N_2 at 296 K and pressure range of 40–250 Torr using SDV profile.

Table 4
N_2-shifting coefficients $\delta^0_{N_2}$ ($cm^{-1}\ atm^{-1}$) at 296 K. Results are derived from the RP, GP, RGP, CR, SDV, SDR, CSDR and VP line-shapes.

Shift ($cm^{-1}\ atm^{-1}$)	P(21)	P(19)	P(16)	R(16)	R(19)	R(21)
RP	−0.0089(1)	−0.0071(2)	−0.0083(1)	−0.0084(1)	−0.0088(1)	−0.0097(1)
GP	−0.0089(1)	−0.0070(2)	−0.0086(1)	−0.0091(1)	−0.0091(1)	−0.0101(1)
RGP	−0.0089(1)	−0.0069(2)	−0.0083(1)	−0.0085(1)	−0.0089(1)	−0.0098(1)
CR	−0.0084(1)	—	−0.0077(1)	−0.0078(1)	−0.0092(2)	−0.0122(1)
SDV	−0.0083(2)	−0.0064(3)	−0.0097(2)	−0.0099(3)	−0.0094(2)	−0.0127(3)
SDR	−0.0072(2)	−0.0055(3)	−0.0089(2)	−0.0010(3)	−0.0093(2)	−0.0130(3)
CSDR	−0.0071(2)	−0.0053(3)	−0.0085(2)	−0.0098(3)	−0.0092(2)	−0.0129(3)
VP	−0.0072(3)	−0.0056(4)	−0.0086(2)	−0.0102(3)	−0.0093(2)	−0.0128(3)

Table 5
N_2-line mixing coefficients (cm^{-1} atm^{-1}) at 296 K. Results are derived from the SDV, SDR and CSDR line-shapes.

Line mixing (cm^{-1} atm^{-1})	P(21)	P(19)	P(16)	R(16)	R(21)
SDV	−0.0192(21)	−0.0687(85)	0.0138(19)	0.0018(18)	0.0354(23)
SDR	−0.0198(21)	−0.0757(85)	0.012(19)	0.0006(18)	0.0337(23)
CSDR	−0.0214(21)	−0.0926(83)	0.009(19)	0.0036(19)	0.0347(23)

on the absorption coefficients at elevated pressures and in the line wings. Introducing the line mixing in the calculations of line-shapes in $\nu_1+\nu_3$ seems to be necessary, since the mentioned line-shape corrections such as broadening, narrowing and shift give dominating effects near the line center, whereas the line wings are generally much less affected. Moreover, after taking line mixing into account, it decreased the discrepancy of experimental data with calculations and made the residuals slightly better as its shown in Fig. 8 for pressure 40–250 Torr. As can be seen from two residuals, for 250 Torr with line mixing effect, the wings are spread closer to zero than the one without line mixing. We were not able to the line mixing effect for the R(19) transition, because at higher pressures this line becomes saturated.

4. Conclusions

This study investigates the effect of using different line-shape models on line parameters (line broadening, pressure induced shift, narrowing and line mixing) for C_2H_2 broadened by N_2 in the $\nu_1+\nu_3$ band. We obtained different line-shape parameters which are needed for describing an observed spectrum. The VP fails to reproduce closely the experimental spectra. In the pressure range 5–40 Torr, the RGP can reproduce the experimental spectra very well. However, this model is symmetric and there remains a small asymmetry in the spectral lines that is not accounted for. This asymmetry is more probably results from speed dependent effects as can be supported by our results for the SDV profile which reproduces the experimental lines in pressure range from 5 to 250 Torr better than mentioned models. In testing speed dependent effect we also considered the effect of line mixing and could deduce values for this parameter.

We also examined the impact of the potential shape on the lines of interest, and selected a value for the parameter q using fits with the SDV, SDR and CSDR models to reproduce better residuals. This study could be extended by using partially correlated models such as the partially Correlated Speed Dependent Rautian (pCSDR) and partially Correlated Speed Dependent Galatry (pCSDG) that may account for the small discrepancies between the profiles obtained experimentally and those obtained using fully correlated models.

Acknowledgments

This work was supported by the Natural Sciences and Engineering Research Council of Canada. We would like to further thank the NSERC CREATE AMETHYST Program at the University of Lethbridge for the continued funding and academic support of our graduate students. We are grateful to D.R. Hurtmans of Universite Libre de Bruxelles for making available to us his line-shape fitting software.

References

[1] Spencer J, Grinspoon D. Planetary science: inside Enceladus. Nature 2007;445:376–7.
[2] Herman M. The acetylene ground state saga. Mol Phys 2007;105:2217–41.
[3] Nguyen L, Blanquet G, Dhyne M, Lepere M. Ne- and Kr-broadening coefficients in the ν_7 band of C_2H_4 studied by diode-laser spectroscopy. J Mol Spectrosc 2009;254:94–8.
[4] Arteaga SW, Bejger CM, Gerecke JL, Hardwick JL, Martin ZT, Mayo J, et al. Line broadening and shift coefficients of acetylene at 1550 nm. J Mol Spectrosc 2007;243:253–66.
[5] Nguyen L, Ivanov SV, Buzykin OG, Buldyreva J. Comparative analysis of purely classical and semiclassical approaches to collision line broadening of polyatomic molecules: II. C2H2–He case. J Mol Spectrosc 2006;239:101–7.
[6] Buldyreva J, Nguyen L. On the role of trajectory modelling in the C_2H_2 infrared line-broadening computation. Mol Phys 2004;102:1523–35.
[7] Buldyreva J, Ivanov SV, Nguyen L. Collisional line broadening in the atmosphere of light particles: problems and solutions in the framework of semiclassical treatment. J Raman Spectrosc 2005;36:148–52.
[8] Ivanov SV, Nguyen L, Buldyreva J. Comparative analysis of purely classical and semiclassical approaches to collision line broadening of polyatomic molecules: I. C_2H_2–Ar case. J Mol Spectrosc 2005;233:60–7.
[9] Thibault F. Theoretical He-broadening coefficients of infrared and Raman C_2H_2 lines and their temperature dependence. J Mol Spectrosc 2005;234:286–8.
[10] Cappelletti D, Bartolomei M, Sabido M, Pirani F, Blanquet G, Walrand J, et al. Collision cross sections, pressure-broadening coefficients and second virial coefficients for the acetylene-argon complex: experiments and calculations on a new potential energy surface. J Phys Chem A 2005;109:8471–80.
[11] Cappelletti D, Bartolomei M, Carmona-Novillo E, Pirani F, Blanquet G, Thibault F. Intermolecular interaction potentials for the Ar–C_2H_2, Kr–C_2H_2, and Xe–C_2H_2 weakly bound complexes: Information from molecular beam scattering, pressure broadening coefficients, and rovibrational spectroscopy. J Chem Phys 2007:126.
[12] Ghosh S, Sharping JE, Ouzounov DG, Gaeta AL. Resonant optical interactions with molecules confined in photonic band-gap fibers. Phys Rev Lett 2005;94:093902.
[13] Rothman LS, Gordon IE, Babikov Y, Barbe A, Chris Benner D, Bernath PF, et al. The HITRAN2012 molecular spectroscopic database. J Quant Spectrosc Radiat Transf 2013;130:4–50.
[14] Jacquinet-Husson N, Scott NA, Chédin A, Crépeau L, Armante R, Capelle V, et al. The GEISA spectroscopic database: current and future archive for Earth and planetary atmosphere studies. J Quant Spectrosc Radiat Transf 2008;109:1043–59.
[15] Mandin JY, Dana V, Claveau C. Line intensities in the ν5 band of acetylene $12C_2H_2$. J Quant Spectrosc Radiat Transf 2000;67:429–46.
[16] Rank DH, Eastman DP, Birtley WB, Wiggins TA. Shapes and breadths of some molecular rotation–vibration band lines perturbed by rare gases. J Chem Phys 1960;33:327–8.
[17] Varanasi P, Bangaru BRP. Intensity and half-width measurements in 1.525 mum band of acetylene. J Quant Spectrosc Radiat Transf 1975;15:267–73.

[18] Pine AS. Self-broadening, N2-broadening and Ar-broadening and line mixing in HCN and C_2H_2. J Quant Spectrosc Radiat Transf 1993;50:149–66.
[19] Rautian SG, Sobel'man II. The effect of collisions on the Doppler broadening of spectral lines. Sov Phys Uspekhi 1967;9:701.
[20] Biswas D, Ray B, Dutta S, Ghosh PN. Diode laser spectroscopic measurement of line shape of ($\nu_1+3\nu_3$) band transitions of acetylene. Appl Phys B: Lasers Opt 1999;68:1125–30.
[21] Über das WV. Gesetz intensitätsverteilung innerhalb der linien eines gasspektrams. Sitzber. Bayr Akad München Ber; 1912. p. 603.
[22] Yelleswarapu C, Sharma A. Pressure-induced self-broadening and frequency shift measurements of absorption lines of acetylene using tunable diode laser absorption spectroscopy. J Quant Spectrosc Radiat Transf 2001;69:151–8.
[23] Povey C, Predoi-Cross A, Hurtmans DR. Line shape study of acetylene transitions in the $\nu_1+\nu_2+\nu_4+\nu_5$ band over a range of temperatures. J Mol Spectrosc 2011;268:177–88.
[24] Povey C, Guillorel-Obregon M, Predoi-Cross A, Ivanov SV, Buzykin OG, Thibault F. Low pressure line shape study of nitrogen-perturbed acetylene transitions in the $\nu_1+\nu_3$ band over a range of temperatures1. Can J Phys 2013:1–10.
[25] Ward J, Cooper J, Smith EW. Correlation Effects in theory of combined Doppler and pressure broadening. 1. Classical theory. J Quant Spectrosc Radiat Transf 1974;14:555–90.
[26] Rozario H, Garber J, Povey C, Hurtmans D, Buldyreva J, Predoi-Cross A. Experimental and theoretical study of N-2-broadened acetylene line parameters in the nu(1)+nu(3) band over a range of temperatures. Mol Phys 2012;110:2645–63.
[27] Valipour H, Zimmermann D. Investigation of J dependence of line shift, line broadening, and line narrowing coefficients in the $\nu_1+3\nu_3$ absorption band of acetylene. J Chem Phys 2001;114:3535–45.
[28] Galatry L. Phys Rev Lett 1961;122:1218.
[29] Jacquemart D, Mandin JY, Dana V, Regalia-Jarlot L, Thomas X, Von der Heyden P. Multispectrum fitting measurements of line parameters for 5-mum cold bands of acetylene. J Quant Spectrosc Radiat Transf 2002;75:397–422.
[30] Li JS, Durry G, Cousin J, Joly L, Parvitte B, Zeninari V. Self-broadening coefficients and positions of acetylene around 1.533 mum studied by high-resolution diode laser absorption spectrometry. J Quant Spectrosc Radiat Transf 2010;111:2332–40.
[31] Fissiaux L, Dhyne M, Lepère M. Diode-laser spectroscopy: pressure dependence of N_2-broadening coefficients of lines in the band of C_2H_2. J Mol Spectrosc 2009;254:10–5.
[32] Lance B, Blanquet G, Walrand J, Bouanich JP. On the speed-dependent hard collision lineshape models: application to C_2H_2 perturbed by Xe. J Mol Spectrosc 1997;185:262–71.
[33] Devi VM, Benner DC, Rinsland CP, Smith MAH, Sidney BD. Tunable diode-laser measurements of N-2- and Air-broadened halfwidths – lines in the (nu-4+nu-5)0 band of (C_2H_2)–C-12 near 7.4 mum. J Mol Spectrosc 1985;114:49–53.
[34] Podolske JR, Loewenstein M, Varanasi P. Diode-laser line strength measurements of the (nu-4+nu-5)0 band of (C_2H_2)–C-12. J Mol Spectrosc 1984;107:241–9.
[35] Lambot D, Blanquet G, Bouanich JP. Diode-laser measurements of collisional broadening in the V5 Band OF C_2H_2 perturbed by O_2 and N_2. J Mol Spectrosc 1989;136:86–92.
[36] Dhyne M, Joubert P, Populaire JC, Lepere M. Collisional broadening and shift coefficients of lines in the nu(4)+nu(5) band of (C_2H_2)–C-12 diluted in N-2 from low to room temperatures. J Quant Spectrosc Radiat Transf 2010;111:973–89.
[37] Cich MJ, McRaven CP, Lopez GV, Sears TJ, Hurtmans D, Mantz AW. Temperature-dependent pressure broadened line shape measurements in the $\nu1+\nu3$ band of acetylene using a diode laser referenced to a frequency comb. Appl Phys B 2012;109:373–84.
[38] Pine AS. Asymmetries and correlations in speed-dependent Dicke-narrowed line shapes of argon-broadened HF. J Quant Spectrosc Radiat Transf 1999;62:397–423.
[39] Dicke RH. The effect of collisions upon the Doppler width of spectral lines. Phys Rev 1953;89:472–3.
[40] Hurtmans D, Dufour G, Bell W, Henry A, Valentin A, Camy-Peyret C. Line intensity of R(0) and R(3) of the $12CH_4$ $2\nu3$ band from diode laser spectroscopy. J Mol Spectrosc 2002;215:128–33.
[41] Hirschfelder JO, Curtiss CF, Bird RB. Molecular theory of gases and liquids. University of Wisconsin; 1964.
[42] Berman PR. Speed-dependent collisional width and shift parameters in spectral profiles. J Quant Spectrosc Radiat Transf 1972;12:1331–42.
[43] Pickett HM. Effects of velocity averaging on the shapes of absorption-lines. J Chem Phys 1980;73:6090–4.
[44] Rohart F, Mader H, Nicolaisen HW. Speed dependence of rotational relaxation induced by foreign gas collisions – studies on CH_3F by millimeter-wave coherent transients. J Chem Phys 1994;101:6475–86.
[45] Rohart F, Nguyen L, Buldyreva J, Colmont JM, Wlodarczak G. Lineshapes of the 172 and 602 GHz rotational transitions of (HCN)–N-15. J Mol Spectrosc 2007;246:213–27.
[46] Joubert P, Bonamy J, Robert D, Domenech JL, Bermejo D. A partially correlated strong collision model for velocity- and state-changing collisions application to Ar-broadened HF rovibrational line shape. J Quant Spectrosc Radiat Transf 1999;61:519–31.
[47] Ngo NH, Lisak D, Trana H, Hartmanna J-M. J Quant Spectrosc Radiat Transf 2013;129:89–100.
[48] Wcislo P, Ciurylo R. J Quant Spectrosc Radiat Transf 2013;120:36–43.
[49] Thibault F, Mantz AW, Claveau C, Henry A, Valentin A, Hurtmans D. Broadening of the R(0) and P(2) lines in the (CO)–C-13 fundamental by helium atoms from 300 K down to 12 K: measurements and comparison with close-coupling calculations. J Mol Spectrosc 2007;246:118–25.
[50] Thompson DR, Chris Benner D, Brown LR, Crisp D, Malathy Devi V, Jiang Y, et al. Atmospheric validation of high accuracy CO_2 absorption coefficients for the OCO-2 mission. J Quant Spectrosc Radiat Transf 2012;113:2265–76.